HHS Public Access

Author manuscript

Clin Biomech (Bristol, Avon). Author manuscript; available in PMC 2017 July 21.

Published in final edited form as:

Clin Biomech (Bristol, Avon). 2017 January ; 41: 20–27. doi:10.1016/j.clinbiomech.2016.11.003.

Pelvic Floor Dynamics During High-Impact Athletic Activities: A Computational Modeling Study

Nicholas Dias[†],
Department of Biomedical Engineering, University of Houston, 360 HBS Building, 4811 Calhoun Rd., Houston, TX, USA 77004

Yun Peng[†],
Department of Biomedical Engineering, University of Houston, 360 HBS Building, 4811 Calhoun Rd., Houston, TX, USA 77004

Rose Khavari,
Department of Urology, Houston Methodist Hospital and Research Institute, 6565 Fannin St, Suite 2100, Houston, TX, USA 77030-2703

Nissrine A. Nakib,
Department of Urology, University of Minnesota, 420 Delaware St. SE MMC 394, Minneapolis, MN, USA 55455-0341

Robert M. Sweet,
Department of Urology, University of Minnesota, 420 Delaware St. SE MMC 394, Minneapolis, MN, USA 55455-0341

Gerald W. Timm,
Department of Urology, University of Minnesota, 420 Delaware St. SE MMC 394, Minneapolis, MN, USA 55455-0341

Arthur G. Erdman,
Department of Mechanical Engineering, University of Minnesota, 111 Church Street SE, Minneapolis, MN, USA 55455-0341

Timothy B. Boone, and
Department of Urology, Houston Methodist Hospital and Research Institute, 6565 Fannin St, Suite 2100, Houston, TX, USA 77030-2703

Yingchun Zhang
Department of Biomedical Engineering, University of Houston, 360 HBS Building, 4811 Calhoun Rd., Houston, TX, USA 77004

Abstract

Background—Stress urinary incontinence is a significant problem in young female athletes, but the pathophysiology remains unclear because of the limited knowledge of the pelvic floor support

Correspondence to: Yingchun Zhang.

[†]Equal contribution

function and limited capability of currently available assessment tools. The aim of our study is to develop an advanced computer modeling tool to better understand the dynamics of the internal pelvic floor during highly transient athletic activities.

Methods—Apelvic model was developed based on high-resolution MRI scans of a healthy nulliparous young female. A jump-landing process was simulated using realistic boundary conditions captured from jumping experiments. Hypothesized alterations of the function of pelvic floor muscles were simulated by weakening or strengthening the levator ani muscle stiffness at different levels. Intra-abdominal pressures and corresponding deformations of pelvic floor structures were monitored at different levels of weakness or enhancement.

Findings—Results show that pelvic floor deformations generated during a jump-landing process differed greatly from those seen in a Valsalva maneuver which is commonly used for diagnosis in clinic. The urethral mobility was only slightly influenced by the alterations of the levator ani muscle stiffness. Implications for risk factors and treatment strategies were also discussed.

Interpretation—Results suggest that clinical diagnosis should make allowances for observed differences in pelvic floor deformations between a Valsalva maneuver and a jump-landing process to ensure accuracy. Urethral hypermobility may be a less contributing factor than the intrinsic sphincteric closure system to the incontinence of young female athletes.

Keywords

Finite Element method; Pelvic Floor Muscle; Urethral Hypermobility; Stress Urinary Incontinence; Female Athletes

1. INTRODUCTION

Stress urinary incontinence (SUI), the involuntary leakage of urine under increased intra-abdominal pressure (IAP), has an observed prevalence of between 4% and 35% [1]. Though SUI is a common problem for elderly and parous women, recent studies showed that SUI is a non-negligible problem in nulliparous female athletes, with the prevalence varying from 12.5% to as high as 80% [2]. SUI in young athletes often goes unreported for fear of embarrassment [3]. It can result in the athlete's modifying her technique, or even completely abandoning the sport and becoming physical inactivity [4].

In the "hammock hypothesis" theory, the levator ani muscle (LAM) plays a significant role in maintaining urinary continence [5]. During an IAP increase, the LAM, a stiff posterior supportive structure, helps the urethral closure by allowing the urethra and other pelvic organs to be tightly compressed against it. Clinical observations found that LAM injuries can lead to a reduced urethral support (urethral hypermobility) [6], which is often associated with SUI. However, significant differences exist between the physiological conditions and environments of young female athletes and those of women in the general population. What these factors contribute to the pathophysiology of SUI remains unclear and warrants further investigation.

First, young female athletes often experience significantly greater and more sudden IAP increases, especially during high-impact activities such as running and jumping [7].

However, existing techniques for SUI diagnosis, including magnetic resonance (MR) imaging [8], perineometry [9], and electromyography [10], are unable to non-invasively characterize the highly transient internal mechanics of the pelvic floor during these activities. Instead, diagnosis is often made on the basis of observations from Valsalva maneuvers [11]. Differences in results obtained with this alternative approach require investigation, in order to ensure the correctness of the corresponding diagnosis.

Second, our knowledge of the pelvic floor muscles (PFMs) of young female athletes is limited. Two existing hypotheses regarding their PFMs are totally opposite: one suggests that female athletes have strong PFMs because of the training stimulus from the co-activation of the abdominal muscle, while the other theory postulates that repeated increases in IAP can cause fatigue and weaken the pelvic floor [12]. To date, no equivocal evidence has been presented to support either one. The effect of neither of these hypothesized alterations in PFM functions on the urethral integrity during the sudden IAP increase could be properly tested.

Computer modeling and simulation provide a potential solution to these challenges in testing. Recent advances in medical imaging allowed the reconstruction of computer models based on high-resolution MR images [13, 14], maximally preserving anatomical integrity and correctness. Computer simulation provides a reliable tool for characterizing dynamic biological processes that are otherwise difficult to observe through traditional techniques [15–24]. Several computer models have been developed to study SUI [15] and pelvic organ prolapse [16, 18], but limited efforts have been made to apply this approach to explore the pathophysiology of SUI in young female athletes [8, 23].

In this study, we presented a complete pelvic model obtained from high-resolution MR images of a young healthy female. The dynamic pelvic floor deformation during a jump-landing process was characterized and compared with the results of a Valsalva maneuver. The effect of the hypothesized alterations in the PFM function on urethral mobility was tested.

2. METHODS

2.1 3D Female Pelvic Floor Modeling

The 3D computational model of the female pelvis used in this study was adopted from previous modeling works [13, 14]. Briefly, T2 weighted MR images of the pelvis of a healthy female (21-year-old, white, Caucasian, nulliparous, nonsmoker, non-athletic, body mass index=22) were obtained axially with a 3T MR imaging scanner (Trio Tim, Siemens, Germany), with a slice thickness of 3mm, matrix of 320 × 160, field of view of 430mm and pixel size of 1.344mm. The images were manually segmented in Mimics (Materialise Group, Leuven, Belgium). Closed-surface 3D geometries were calculated from the segmentation results for each pelvic floor component and then smoothed in MAYA 8.5 (Autodesk, Inc., San Rafael, CA, USA) and Rhinoceros 4.0 (McNeel North America, Seattle, WA, USA) for artifact and intersections removal. The smoothed geometries were then imported into ABAQUS 6.12 (SIMULIA, Providence, RI, USA) for tetrahedral element discretization. Segmentation and smoothing were performed under the guidance of an

experienced urologist to minimize errors between the reconstructed model and original MR images. The final model consisted of 44 parts in 61,867 elements, as shown in Figure 1. Essential pelvic floor components including the pelvic floor muscles, bladder, vagina, uterus, rectum, ligaments, etc. were included to maximally maintain the integrity of the female pelvic anatomy. A specially-designed bodyfill part was used to represent the intra-abdominal contents and to allow the transmission of IAP during athletic activities. This modeling approach has been validated using dynamic MR imaging in our previous study [13].

2.2 Contacts, Interactions and Boundary Conditions

Anatomical connections between soft tissues were imposed using the ABAQUS “surface-to-surface” tie constraint option, which couples the motion of nodes from two parts that are anatomically bound. Interactions between tissues that are not anatomically connected were defined using the ABAQUS “general contact” algorithm, which allows parts to interact with each other with a defined interaction behavior and resist unrealistic surface intersections. Pelvic ligaments (cardinal, uterosacral and pubourethral ligaments) were modeled using connector elements with an axial elastic behavior [18]. A vertical jump was simulated in this study to induce the high-impact effect, as previous studies found a higher prevalence of SUI in young female athletes whose activities involve jumping [25]. Realistic boundary conditions were set using velocity recordings from accelerometer (Crossbow Technology, Inc., San Jose, CA). In the jump experiment, the subject jumped from a 30 cm box and landed on a hardwood floor. This height can fairly reflect the typical vertical jumping heights of collegiate female ball game players [26]. The accelerometer sensor was placed on the skin directly above the iliac crest, as data captured above the approximate location of the iliac crest on the left and right lower back proved to be the most reliable [27]. During the jump process, the entire body first falls freely in the air, accelerating all body tissues uniformly because of gravity. No relative motions exist during this phase. Upon the initiation of landing (when both feet touch the ground), the bony pelvis starts to decelerate gradually because of the combined effect of inertia and the buffering effect from lower limbs. The sensor placed on the iliac crest most accurately records the motions of the bony pelvis during this process. Meanwhile, soft tissues interact with pelvic bones because of the difference in velocities and pelvic floor contents start to show deformation because of this interaction. Thus, the landing phase provides the most critical information to characterize the deformations of pelvic floor structures. The velocity recorded during the landing phase, as shown in Figure 2, was assigned as boundary conditions to the reference point that controlled the motion of the pelvic bones and to the bottom surface of the model, as shown in Figure 1c. The initial velocity upon the initiation of landing was set to move in vertical direction at 2.81 m/s and in the horizontal direction at 0.29 m/s according to the accelerometer readings.

2.3 Material Properties

Although biological soft tissues demonstrate viscoelastic properties [17, 28–30], previous studies have found a quasi-linear material property of urological soft tissues when the stress level is under 70% of the maximal stress value [24]. Consequently, elastic material properties were used to represent mechanical behaviors of soft tissues. Most soft tissues

were modeled as linear elastic materials [13, 14], as it has been found that linear elasticity produces a displacement field similar to that produced using nonlinear elasticity, while benefiting the computation efficiency [19]. However, to better characterize the behaviors of the bladder and LAM, hyperelastic models were adopted [16, 31]. The pelvic bone was modeled as a rigid body because of its much greater stiffness than soft tissues [15]. Table 1 summarizes the constitutive models used for soft tissues within this study.

Published literature postulates that PFM in athletes could be either strengthened or weakened [12]. Our model simulated the hypothesized weakness or enhancement of pelvic floor muscles by multiplying the uniaxial stress-strain data of the LAM with a scaling coefficient [15]. The resulting stress-strain data was then used as the altered mechanical properties of the LAM, as shown in Figure 3.

2.4 Design of Simulations

A total of nine tests were performed. Table 2 summarizes the plan of simulations conducted in this study. In the control test, there was no enhancement or impairment of the LAM. In the weakening tests, impairments of 25%, 50%, 75% and 95% were simulated using a scaling coefficient of 0.75, 0.5, 0.25, and 0.05, respectively. In the strengthening tests, enhancements of 25%, 50%, 75% and 100% were simulated using a scaling coefficient of 1.25, 1.50, 1.75 and 2.00.

In each test, the bladder neck displacement in the sagittal plane and the urethral excursion angle (clinically equivalent with Q-tip rotational angle) were used as metrics to assess the urethral hypermobility [13, 14]. Definitions of these two metrics are shown in Figure 1. The IAP, calculated as the contact pressure between the inner bladder wall and the urine, was also reported. All of these metrics were monitored dynamically throughout the simulation time using ABAQUS history and field output request functions. The computation was conducted in parallel processing with an AMD Cluster (Maxwell, 8 cores on 2 CPUs: 16 nodes total, 2GB RAM) in the Center for Advanced Computing and Data Systems at the University of Houston. On average, it took about 5 hours for the Maxwell cluster to complete 1 computation task.

3. RESULTS

The simulation results showed that the pelvic floor deformation during a jump landing process demonstrated two stages (Figure 4). During stage one, the pelvic floor showed a “leaning forward compression”. Compared with the resting state configuration (Figure 4a), the bladder was compressed against the decelerating pubic bone and stretched anteroposteriorly (Figure 4b). The frontal bladder leaned forward partly because of the compression and partly because of the initial horizontal velocity. At the end of stage one, the bladder was maximally compressed against the front bodyfill part with all of its kinetic energy converted to the elastic potential energy. During stage two, the bladder started to “bounce back” because of the release of the stored elastic potential energy and to develop posterior deformations further differing from the resting state, as shown in Figure 4c. Supports were provided by the posterior compartments (vaginal wall and LAM) to counterbalance the excessive posterior motions (hypermobility).

For the control test, the IAP reached a first peak of 194.6 cmH_2O at 0.064 seconds. A second peak of 114.1 cmH_2O was found at 0.136 seconds. A maximum bladder neck displacement of 12.1 mm and a maximum urethral excursion angle of 22.9° were found in the control test, both occurring at a time instance close to the second IAP peak. Table 2 summarizes the results for all tests. Altering the LAM stiffness caused only slight differences in the two peak IAPs (all less than 4%). The differences in the maximum bladder neck displacement ranged from −0.2 mm to +1.6 mm and in the maximum urethra excursion angles from −2.8° to 2.0°.

4. DISCUSSION

In this study, we developed awhole-pelvic model from a healthy nulliparous female subject and used it to describe the deformations of pelvic floor structures during the jump-landing process and test the effects of altered LAM stiffness on the urethral mobility metrics.

4.1 Comparison with the Valsalva Maneuver

A separate Valsalva simulation was performed using the method described in a previous simulation study [13, 14]. Our simulation showed that the deformations of pelvic floor structures during the jump-landing process differed greatly from that produced in the Valsalva maneuver. The obtained IAP history and the deformation of pelvic floor structures at the maximal IAP were compared. First, at the maximal IAP, the deformation pattern in jump-landing was both anterior and posterior because of the compression against the pelvic bone (Figure 4b and 5a), while in the Valsalva maneuver, the deformations were presented more in an inferoposterior direction (Figure 5b). This is consistent with our preliminary simulation observations [32], and can be explained by the directions of the efforts applied. In jump-landing, the deformation was largely due to the vertical compression of the organs against the pelvic bone, while in straining activities, the effort was oriented at 45 degrees with respect to horizontal axis, from anterior to posterior direction [19]. Second, there was a distinct difference in the history of the IAP development, as seen in Figure 5c. Unlike the Valsalva maneuver, which only produced one single IAP increase [13], the jump-landing process produced two IAP peaks (Figure 6a). The first peak can be explained by the intensifying compression between the free falling soft tissues and the decelerating pubic bone during the falling stage, and was evidenced by the simultaneous occurrence of the maximum IAP (Figure 6a) and the maximum deceleration (Figure 2b) around 0.07 seconds. The second peak can be explained by the “bouncing back” motion of the bladder during stage two. The bladder was compressed horizontally against the vaginal wall and the LAM and thus caused the contact pressure between the inner bladder wall and the urine to increase. This was evidenced by the simultaneous occurrence of the maximal urethral mobility with the second IAP peak around 0.14 seconds. Third, in terms of the IAP magnitude, the maximal IAP observed in the jump landing simulation (194.5 cmH_2O) was much higher than Valsalva simulation results (Figure 5c) or clinical recordings [33]. This IAP value was consistent with pressure readings obtained from previous tests using a transurethral bladder catheter (232 ± 66 cmH_2O) [33].

Because of the challenging nature of performing internal imaging tasks during high-impact athletic activities, Valsalva maneuvers are often used alternatively to assess the pelvic floor dynamics of young female athletes [11]. Our simulation results showed that differences exist in terms of IAP development, IAP peak values and pelvic floor deformation patterns. Clinical diagnosis should make allowances for these differences to ensure accuracy.

4.2 Relation to the Risk Factors for SUI

We found that the effect of weakened LAM stiffness on the proposed urethral hypermobility metrics was minor. The displacement and urethral rotation were increased by only 1.6 mm (13%) and 2° (9%). They differed from common clinical observations: Kruger el. al found that athletes showed greater bladder neck descent on maximal Valsalva maneuver when compared with the control group [11]. Previous simulation results showed that LAM impairment highly impacts the urethral excursion angle on Valsalva maneuver [13]. A possible explanation for this difference is that the previous studies focused on the Valsalva maneuver, while our model examines the urethral excursion during a jump landing. These activities are quite different in nature - Valsalva produces a slow and steady increase in intra-abdominal pressure, while a jump landing results in an intra-abdominal pressure that is strong but transient. The directions of pressure loads in these two activities on pelvic organs are also distinct, as described in Section 4.1. Combined together, these factors made urethral hypermobility a noticeable observation in Valsalva but less obvious during landing a jump. These differences suggested that, during jump-landing, the female pelvic floor reacts to the sudden IAP increase quite differently from the way commonly seen in daily pressure activities. This finding downplayed the role of the weakened LAM stiffness as an etiological factor of the weakened urethral closure functions in young female athletes.

What remains unanswered is what puts the young female athlete at risk for developing SUI. Ashton-Miller and DeLancey explained the urinary continence mechanism through two systems: the intrinsic sphincteric closure system, formed by the urethral sphincteric muscles, and the urethral support system, formed by pelvic floor muscles and connective tissues [34]. Although the pelvic floor can effectively balance the sharp IAP increase during athletic activities to avoid urethral hypermobility, this increases may exceed the capability of the intrinsic closure system. The intrinsic sphincteric closure system seems to contribute more to the maintenance of continence. This may explain why many athletes reported leakage only during athletic activities but not in daily life.

To further explore the risk factors for weakened urethral closure functions in young female athletes, attention should be focused on the characterization of the strength of the urinary sphincteric closure system and, for severe cases, on the neurogenic impairment of urinary sphincter muscles. Preventative actions should also be directed towards enhancing the urethral closure functions.

4.3 Relation to the Pelvic Floor Muscle Training

Pelvic floor muscle training has been shown to be effective at treating SUI for the general population [35]. A recent study also evidenced the effect of pelvic floor muscle training on incontinence of young nulliparous female athletes (N=7) [36]. As one hypothesis was that

athletes have strong pelvic floor muscles because of training stimulus, we tested the effect of enhanced LAM stiffness on urethral mobility. The results showed that the effect of enhanced LAM stiffness on urethral mobility metrics was not remarkable: the maximum bladder neck displacement was lowered by 1 mm (8%) and the urethral excursion angle by 2.8° (12%). These results suggested that the enhanced stiffness of LAM does not reduce the urethral mobility. A possible explanation for weakened urethral closure function in athletes is the repeated stretching of the pudendal nerve in response to repeated instances of substantially increased intra-abdominal pressure. Previous studies have correlated a state of chronic increased intra-abdominal pressure in obese patients with a weak urethra and urinary incontinence [37]. Considering the broad benefits of pelvic floor muscle training, we should not be discouraged by the findings presented in this paper. On one hand, in addition to increased muscle stiffness, pelvic floor muscle training also means a conscious pre-contraction of PFM during physical stress and a muscle volume increase [38, 39]. These changes are found to benefit the maintenance of continence and provide opportunities for future computer simulation work. On the other hand, the observed limited impact of LAM stiffness on the reduction in urethral mobility would otherwise help redirect the focus of physical therapists towards more efficient biometrics in assessing the urethral integrity in young female athletes.

4.4 Limitations and Future Research

One limitation is that we only studied the effects of altered LAM stiffness. Athletes may also demonstrate increased muscle thickness and diameter, and elevated bladder and rectum [11, 38]. These anatomical changes should also be considered to ensure the complete characterization of the pelvic floor structures of young female athletes. With the convenience in MR imaging and computer modeling, these morphological factors can be included in future studies. Another limitation of this study is the lack of statistical power, as the results reported in the study are achieved based on one single pelvic model constructed from one particular subject's MRI data. Efforts will be taken in the future to perform this study based on multiple subjects' pelvic models to take into account the effects of the pelvic anatomy variations on simulation results.

5. CONCLUSIONS

The computational modeling and simulation approach is a useful tool for studying the highly-transient pelvic floor dynamics. We found that pelvic floor deformed distinctly during jump-landing and Valsalva. Clinical diagnosis should make allowances for differences between the pelvic floor deformations in a Valsalva maneuver and those in a jump-landing process to ensure accuracy. We also found that altered LAM stiffness caused only slight changes in urethral mobility, suggesting that urethral hypermobility may be less dominant than expected as a factor causing weakened urethral functions and SUI in young female athletes. Future studies are encouraged to investigate the function of the intrinsic urethral closure system.

Acknowledgments

FUNDING

This work was supported in part by National Institute of Health (NIH) DK082644 and the University of Houston.

References

1. Luber KM. The definition, prevalence, and risk factors for stress urinary incontinence. Reviews in urology. 2004; 6(Suppl 3):S3.
2. Almousa S, Moser H, Kitsoulis G, Almousa N, Tzovaras H, Kastani D. The prevalence of urine incontinence in nulliparous female athletes: a systematic review. Physiotherapy. 2015; 101:e58.
3. Hägglund D, Wadensten B. Fear of humiliation inhibits women's care-seeking behaviour for long-term urinary incontinence. Scandinavian journal of caring sciences. 2007; 21(3):305–312. [PubMed: 17727542]
4. Salvatore S, Serati M, Laterza R, Uccella S, Torella M, Bolis P. The impact of urinary stress incontinence in young and middle-age women practising recreational sports activity: an epidemiological study. British journal of sports medicine. 2009; 43(14):1115–1118. [PubMed: 18819959]
5. DeLancey JO. Structural support of the urethra as it relates to stress urinary incontinence: the hammock hypothesis. American journal of obstetrics and gynecology. 1994; 170(6):1713–1723. [PubMed: 8203431]
6. DeLancey JO. Fascial and muscular abnormalities in women with urethral hypermobility and anterior vaginal wall prolapse. American journal of obstetrics and gynecology. 2002; 187(1):93–98. [PubMed: 12114894]
7. Goldstick O, Constantini N. Urinary incontinence in physically active women and female athletes. British journal of sports medicine. 2014; 48(4):296–298. [PubMed: 23687004]
8. Da Roza T, Brandão S, Oliveira D, Mascarenhas T, Parente M, Duarte JA, Jorge RN. Football practice and urinary incontinence: relation between morphology, function and biomechanics. Journal of biomechanics. 2015
9. da Silva Borin LCM, Nunes FR, de Oliveira Guirro EC. Assessment of pelvic floor muscle pressure in female athletes. Pm&r. 2013; 5(3):189–193. [PubMed: 23122895]
10. Luginbuehl H, Naeff R, Zahnd A, Baeyens J-P, Kuhn A, Radlinger L. Pelvic floor muscle electromyography during different running speeds: an exploratory and reliability study. Archives of gynecology and obstetrics. 2015:1–8.
11. Kruger J, Dietz H, Murphy B. Pelvic floor function in elite nulliparous athletes. Ultrasound in obstetrics & gynecology. 2007; 30(1):81–85. [PubMed: 17497753]
12. Bø K. Exercise and Pelvic Floor Dysfunction in Female Elite Athletes. Handbook of Sports Medicine and Science: The Female Athlete. 2015:76–85.
13. Peng Y, Khavari R, Nakib NA, Boone TB, Zhang Y. Assessment of urethral support using MRI-derived computational modeling of the female pelvis. International urogynecology journal. 2016; 27(2):205–212. [PubMed: 26224383]
14. Peng Y, Khavari R, Nakib NA, Stewart JN, Boone TB, Zhang Y. The single-incision sling to treat female stress urinary incontinence: a dynamic computational study of outcomes and risk factors. Journal of biomechanical engineering. 2015; 137(9):091007.
15. Brandão S, Parente M, Mascarenhas T, da Silva ARG, Ramos I, Jorge RN. Biomechanical study on the bladder neck and urethral positions: Simulation of impairment of the pelvic ligaments. Journal of biomechanics. 2015; 48(2):217–223. [PubMed: 25527889]
16. Chen Z-W, Joli P, Feng Z-Q, Rahim M, Pirró N, Bellemare M-E. Female patient-specific finite element modeling of pelvic organ prolapse (POP). Journal of biomechanics. 2015; 48(2):238–245. [PubMed: 25529137]
17. Dai Z, Peng Y, Mansy HA, Sandler RH, Royston TJ. Comparison of poroviscoelastic models for sound and vibration in the lungs. Journal of vibration and acoustics. 2014; 136(5):050905.
18. Luo J, Chen L, Fenner DE, Ashton-Miller JA, DeLancey JO. A multi-compartment 3-D finite element model of rectocele and Its interaction with cystocele. Journal of biomechanics. 2015
19. Mayeur O, Witz J-F, Lecomte P, Brieu M, Cosson M, Miller K. Influence of geometry and mechanical properties on the accuracy of patient-specific simulation of women pelvic floor. Annals of biomedical engineering. 2015:1–11. [PubMed: 25527321]

20. Wang S, Zhou Y, Tan J, Xu J, Yang J, Liu Y. Computational modeling of magnetic nanoparticle targeting to stent surface under high gradient field. Computational mechanics. 2014; 53(3):403–412. [PubMed: 24653546]
21. Zhang H, Nussbaum MA, Agnew MJ. A new method to assess passive and active ankle stiffness during quiet upright stance. Journal of Electromyography and Kinesiology. 2015; 25(6):937–943. [PubMed: 26547842]
22. Zhang H, Nussbaum MA, Agnew MJ. Development of a sliding mode control model for quiet upright stance. Medical engineering & physics. 2016; 38(2):204–208. [PubMed: 26810735]
23. Zhang Y, Kim S, Erdman AG, Roberts KP, Timm GW. Feasibility of using a computer modeling approach to study SUI induced by landing a jump. Annals of biomedical engineering. 2009; 37(7): 1425–1433. [PubMed: 19415493]
24. Zhang Y, Sweet RM, Metzger GJ, Burke D, Erdman AG, Timm GW. Advanced finite element mesh model of female SUI research during physical and daily activities. Stud Health Technol Inform. 2009; 142:447–452. [PubMed: 19377205]
25. Jácome C, Oliveira D, Marques A, Sá-Couto P. Prevalence and impact of urinary incontinence among female athletes. International Journal of Gynecology & Obstetrics. 2011; 114(1):60–63. [PubMed: 21571270]
26. Dalrymple KJ, Davis SE, Dwyer GB, Moir GL. Effect of static and dynamic stretching on vertical jump performance in collegiate women volleyball players. The Journal of Strength & Conditioning Research. 2010; 24(1):149–155. [PubMed: 20042927]
27. Luginbuehl H, Greter C, Gruenenfelder D, Baeyens J, Kuhn A, Radlinger L. Intra-session test–retest reliability of pelvic floor muscle electromyography during running. International urogynecology journal. 2013; 24(9):1515–1522. [PubMed: 23361854]
28. Wang Q, Zeng H, Best TM, Haas C, Heffner NT, Agarwal S, Zhao Y. A mechatronic system for quantitative application and assessment of massage-like actions in small animals. Annals of biomedical engineering. 2014; 42(1):36–49. [PubMed: 23943071]
29. Zhou D, Peng Y, Bai J, Rosandich RG. CONTACT EFFECT EVALUATION USING STRESS DISTRIBUTION IN VISCOELASTIC MATERIAL UNDER GENERALIZED LOADING. International Journal of Modelling and Simulation. 2014; 34(4)
30. Zhang J, Koo B, Subramanian N, Liu Y, Chattopadhyay A. An optimized cross-linked network model to simulate the linear elastic material response of a smart polymer. Journal of Intelligent Material Systems and Structures. 2015 1045389X15595292.
31. Krcmar, M., Krofta, L., Urbankova, I., Reisl, JF., Havelkova, L., Hyncik, L. INTERNATIONAL UROGYNECOLOGY JOURNAL. SPRINGER LONDON LTD 236 GRAYS INN RD; 6TH FLOOR, LONDON WC1X 8HL, ENGLAND: 2015. BIOMECHANICAL PROPERTIES OF LEVATOR ANI MUSCLE USED FOR VIRTUAL MODEL OF PELVIC FLOOR; p. S163-S164.
32. Peng, Y., Khavari, R., Stewart, J., Boone, T., Zhang, Y. NEUROUROLOGY AND URODYNAMICS. WILEY-BLACKWELL; 111 RIVER ST, HOBOKEN 07030-5774 NJ USA: 2015. COMPARISON OF FEMALE PELVIC FLOOR DEFORMATION BETWEEN JUMPING AND VALSALVA MANEUVER; p. S7-S7.
33. Cobb WS, Burns JM, Kercher KW, Matthews BD, Norton HJ, Heniford BT. Normal intraabdominal pressure in healthy adults. Journal of Surgical Research. 2005; 129(2):231–235. [PubMed: 16140336]
34. ASHTON-MILLER JA, DeLANCEY J. Functional anatomy of the female pelvic floor. Annals of the New York Academy of Sciences. 2007; 1101(1):266–296. [PubMed: 17416924]
35. Bø K. Pelvic floor muscle training in treatment of female stress urinary incontinence, pelvic organ prolapse and sexual dysfunction. World journal of urology. 2012; 30(4):437–443. [PubMed: 21984473]
36. Da Roza T, de Araujo MP, Viana R, Viana S, Jorge RN, Bø K, Mascarenhas T. Pelvic floor muscle training to improve urinary incontinence in young, nulliparous sport students: a pilot study. International urogynecology journal. 2012; 23(8):1069–1073. [PubMed: 22552685]
37. Noblett K, Jensen J, Ostergard D. The relationship of body mass index to intra-abdominal pressure as measured by multichannel cystometry. International Urogynecology Journal. 1997; 8(6):323–326.

38. Brækken IH, Majida M, Engh ME, Bø K. Morphological changes after pelvic floor muscle training measured by 3-dimensional ultrasonography: a randomized controlled trial. Obstetrics & Gynecology. 2010; 115(2 Part 1):317–324. [PubMed: 20093905]

39. Bø K. Pelvic floor muscle training is effective in treatment of female stress urinary incontinence, but how does it work? International Urogynecology Journal. 2004; 15(2):76–84.

40. Haridas B, Hong H, Minoguchi R, Owens S, Osborn T. PelvicSim—A computational-experimental system for biomechanical evaluation of female pelvic floor organ disorders and associated minimally invasive interventions. Stud Health Technol Inf. 2006; 119:182–187.

41. Yamada H, Evans FG. Strength of biological materials. 1970

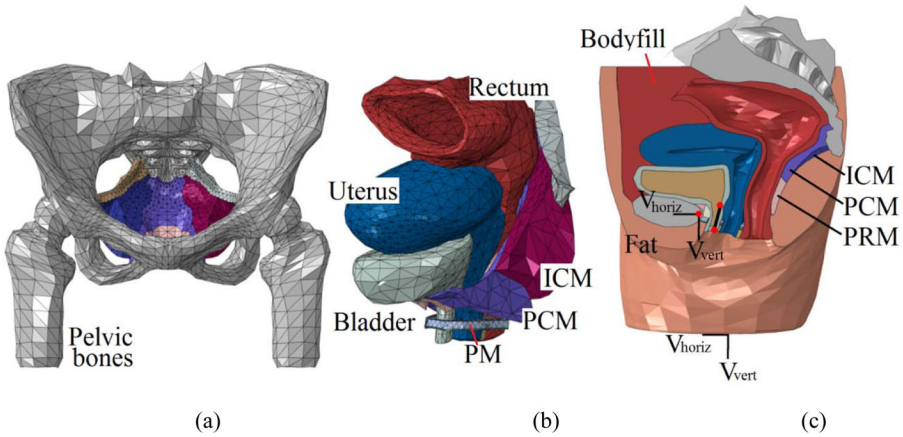

Figure 1.

(a) front view of the pelvic floor muscles and pelvic bone, (b) anterolateral view of the pelvic floor organs and muscles and (c) mid-sagittal view of the complete pelvic model. The velocity boundary conditions are assigned to entire bottom surface and the control point of the rigid bone (represented by the left red spot). The two reference points along the urethra were used to define the urethral excursion angle. Abbreviation used in this figure: ICM–Iliococcygeus muscle, PCM–pubococcygeus muscle, PRM–puborectalis muscle and PM–perineal membrane.

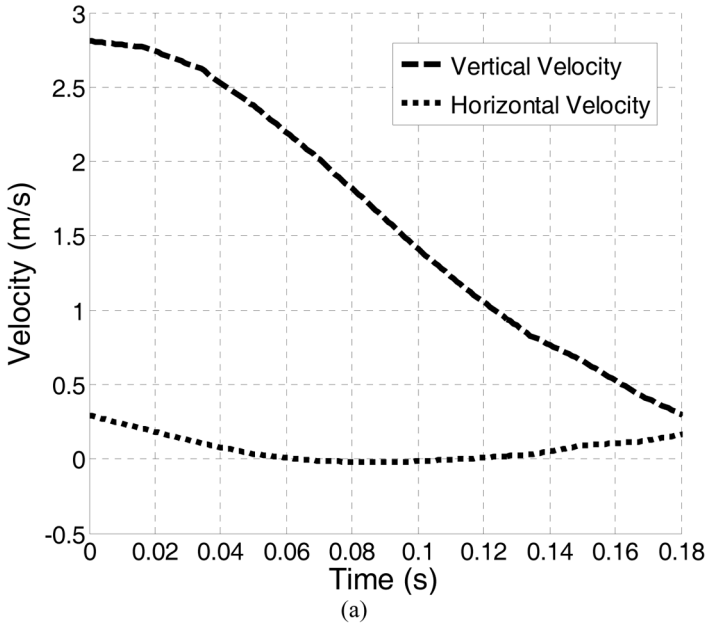

(a)

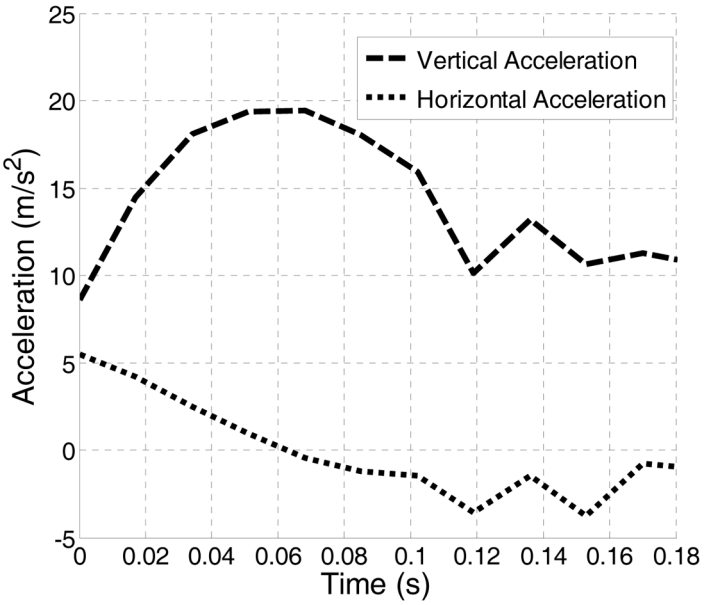

(b)

Figure 2.

(a) horizontal and vertical velocity boundary conditions recorded from jump experiment and (b) corresponding acceleration history.

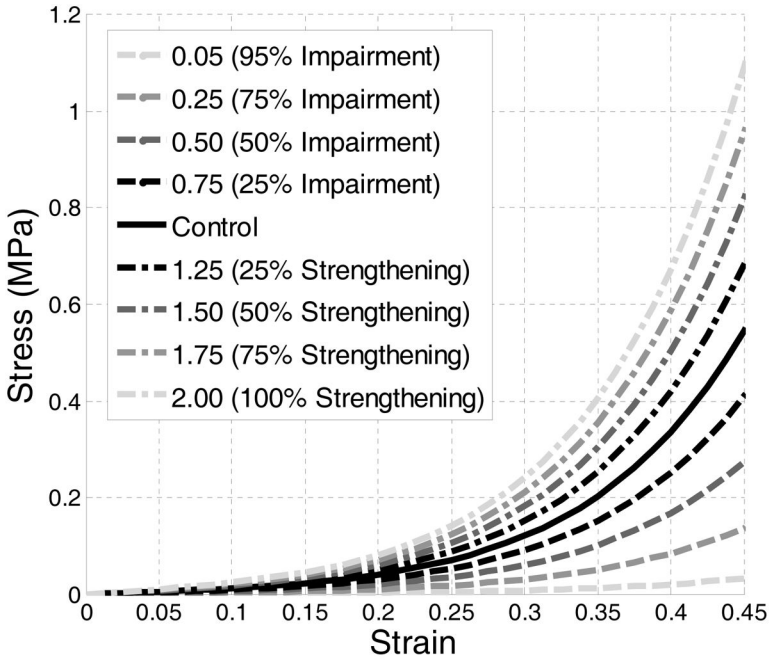

Figure 3.
Stress-strain curves of the intact, impaired and strengthened levator ani muscle.

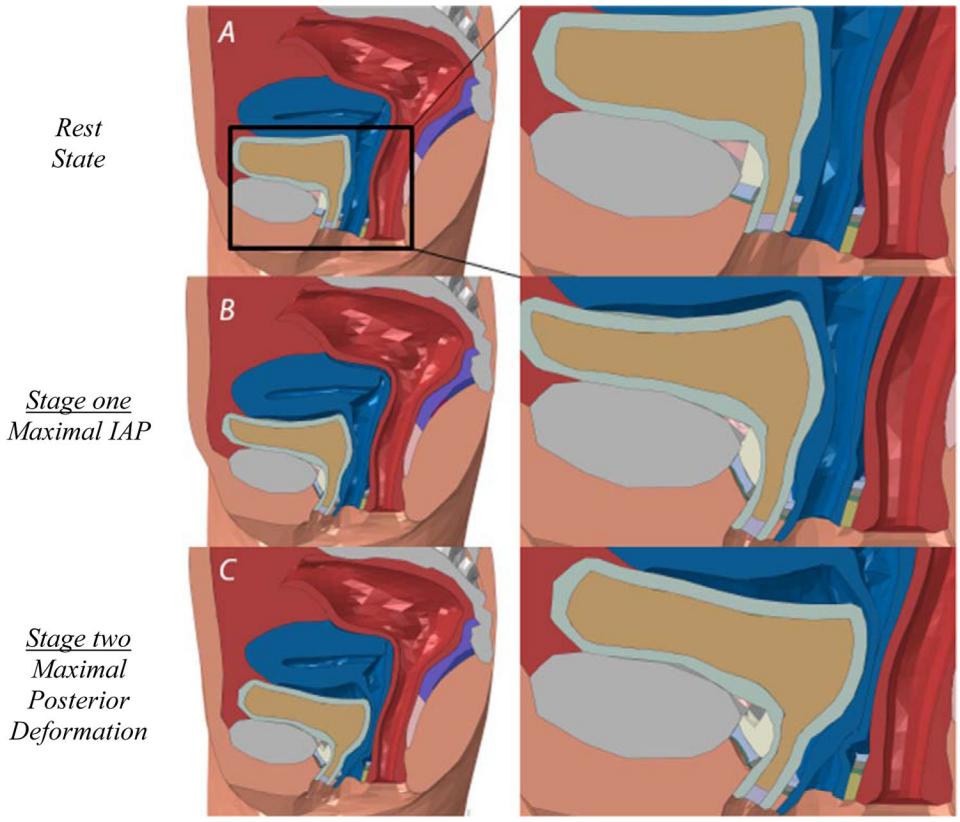

Figure 4.
Pelvic floor configurations at the (a) rest state, (b) maximal IAP and (c) maximal posterior deformation.

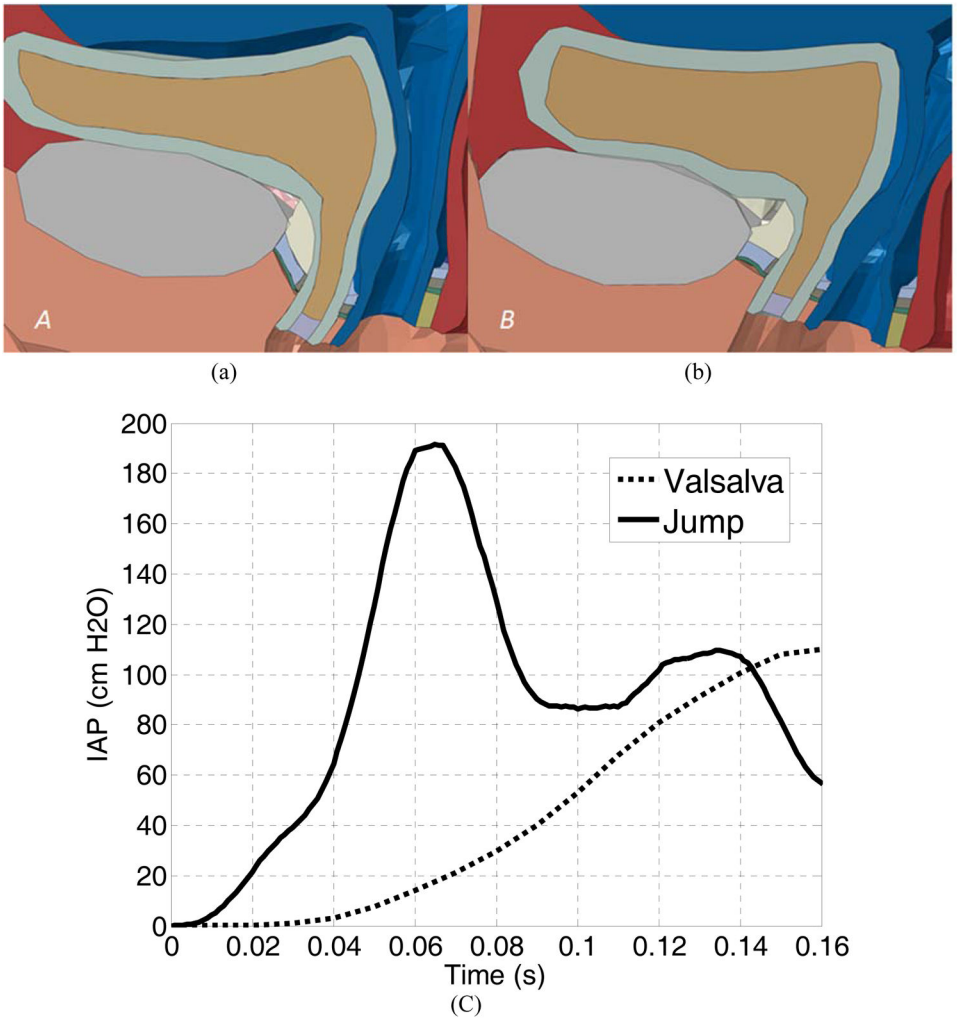

Figure 5.

The comparison of the pelvic floor deformations between (a) jumping and (b) Valsalva at maximal IAP. The comparison of the IAP history plots of jumping and Valsalva was shown in (c).

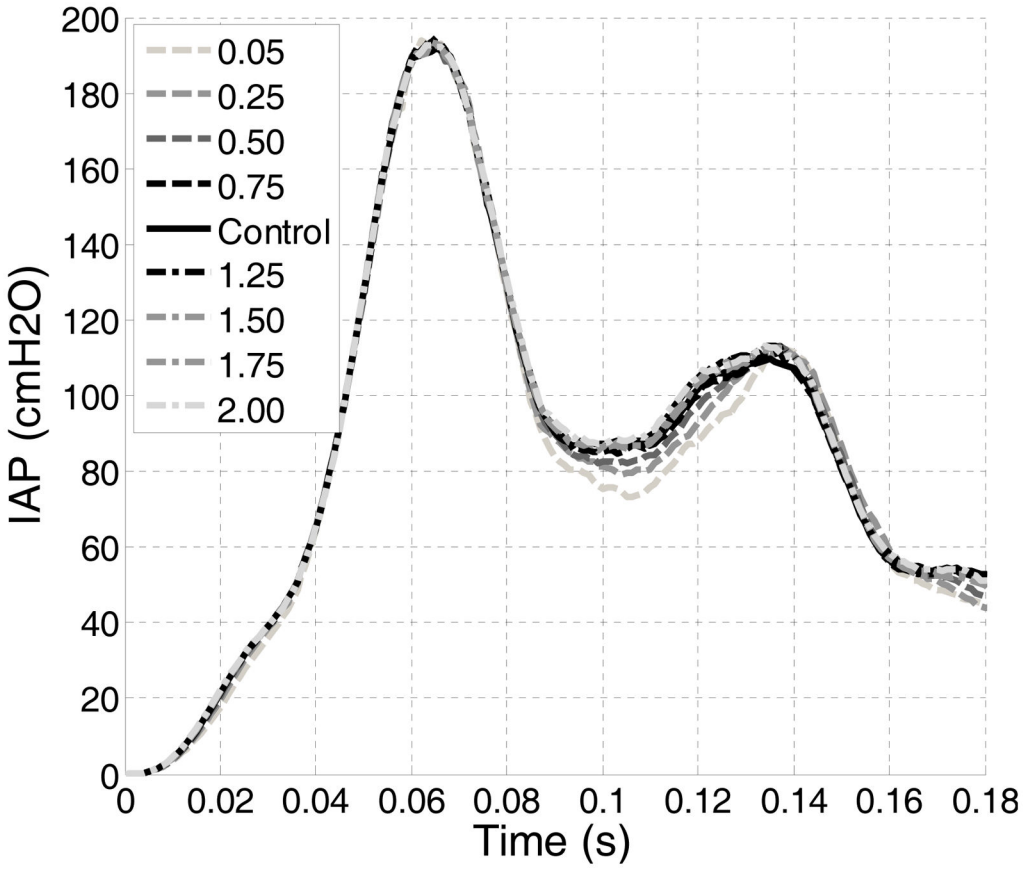

(a)

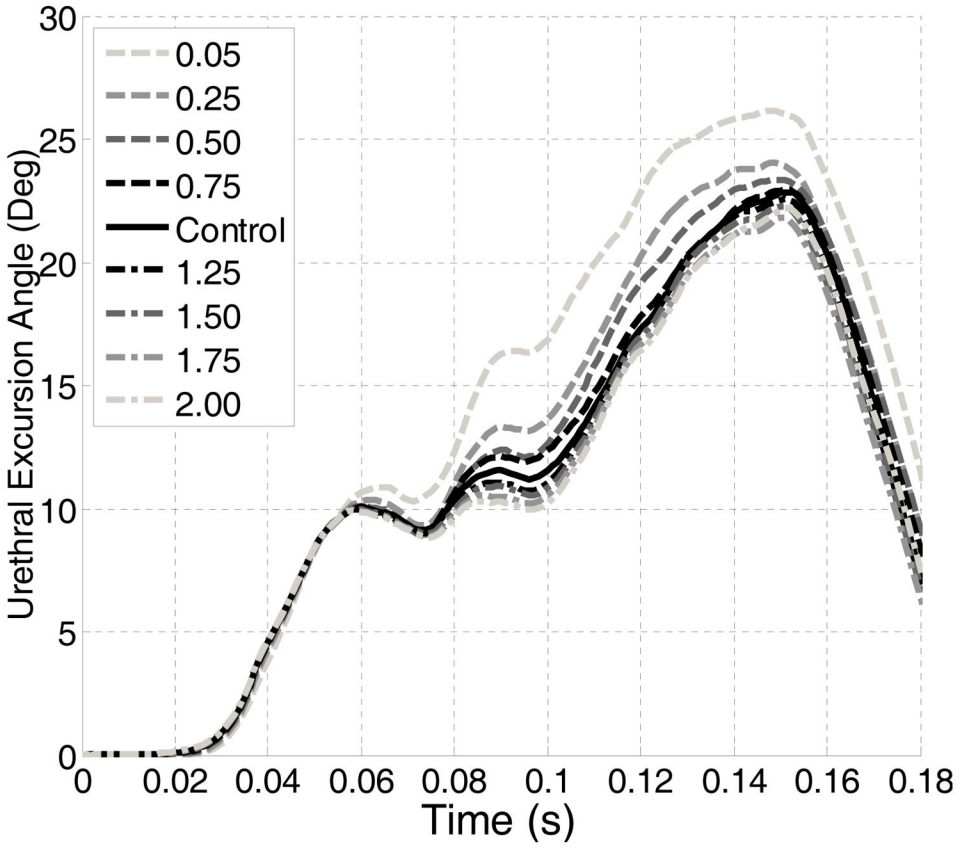

(b)

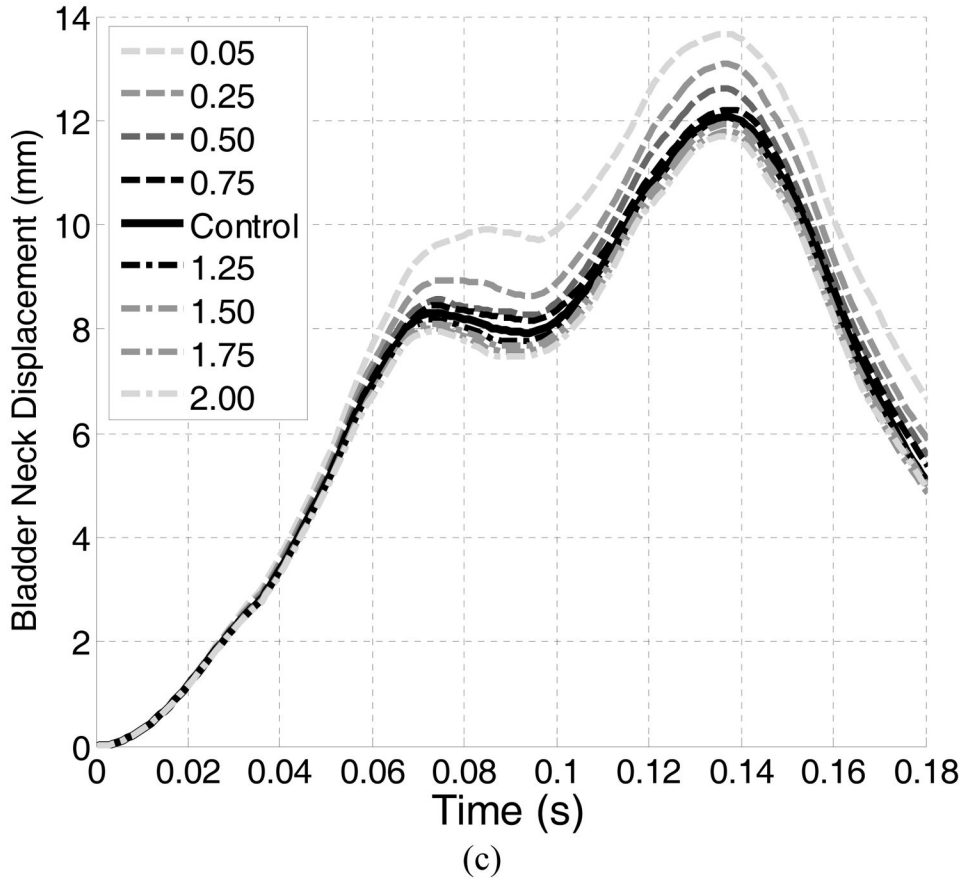

(c)

Figure 6.

Plots of the evolutions of the (a) Intra-abdominal pressure, (b) urethral excursion angle and (c) bladder neck displacement.

Table 1

Material properties for the soft tissues included in the model

Structures	Material Constants		Constitutive Models	Sources
Linear elastic structures	***Young's modulus* (MPa)**	***Poisson's ratio***		
Vagina and uterus	0.005	0.49		
Rectum	0.1	0.49		
Fat	0.05	0.49	Hooke	Ref [40, 41]
Bodyfill	0.05	0.49		
Muscles (excluding LAM)	2.4	0.49		
Urine	1.0e-3	0.49		Ref [13]
Hyperelastic structures				
Levator ani muscle	μ_1 = 0.0082 MPa μ_2 = 0.0216 MPa	α_1 = 0.1803 α_2 = 15.112	Ogden (N = 2)	Ref [31]
Bladder and urethra	C_{10} = 0.071 MPa C_{20} = 0.202 MPa C_{30} = 0.048 MPa		Yeoh	Ref [16]
Others				
Pelvic ligaments	Axial elasticity = 0.15 N/mm *		Hooke	Ref [18]
Pelvic bones	Rigid		Rigid body	Ref [15]

* linearized

Table 2

Plan of simulations and results

Test #	Impairment or Enhancement (%)	Scaling Coefficients	First Peak IAP (cmH_2O)	Second peak IAP (cmH_2O)	Maximum Bladder neck displacement (mm)	Maximum urethral excursion angle (°)
Control						
C0	0	1.00	191.5	109.6	12.1	22.9
Weakened						
1	25	0.75	193.5 (+2.0) *	112.3 (+2.7)	12.2 (+0.1)	22.9 (+0.0)
2	50	0.50	193.2 (+1.7)	112.9 (+3.3)	12.6 (+0.5)	23.3 (+0.4)
3	75	0.25	193.5 (+2.0)	112.4 (+2.8)	13.1 (+1.0)	24.0 (+1.1)
4	95	0.05	193.7 (+2.2)	112.3 (+2.7)	13.7 (+1.6)	24.9 (+2.0)
Strengthened						
1	25	1.25	194.6 (+3.1)	113.2 (+3.6)	11.9 (−0.2)	22.3 (−0.6)
2	50	1.50	193.8 (+2.3)	112.7 (+3.1)	11.6 (−0.5)	21.9 (−1.0)
3	75	1.75	193.3 (+1.8)	112.7 (+3.1)	11.2 (−0.9)	21.1 (−1.8)
4	100	2.00	192.8 (+1.3)	112.9 (+3.3)	11.1 (−1.0)	20.1 (−2.8)

* Number in bracket represents the amount of change from the control test, applies to all